# GEANT4 Simulation of the GTAF

Chong ZOU [1,2], Guangyuan LUAN [1], Haotian LUO [1], Qiwei ZHANG[1*], Jie REN[1], Hongyi WU[1], Xichao RUAN[1*], Hanxiong HUANG[1], Zhaohui WANG[1], Guozhu HE[1], Jie BAO[1], Qi SUN[1], Xiaoyu WANG[1], Mengxiao KANG[1], Jincheng WANG[1], Yingyi LIU[1], Haolan YANG[1] & Xuanbo CHEN[1]

## Affiliations:

[1] Key Laboratory of Nuclear Data, China Institute of Atomic Energy, Beijing 102413 China

[2] China Shipbuilding Trading Co., Ltd., Beijing 100044 China

## * Correspondence author:

Qiwei Zhang *E-mail address:* zqwvictor@126.com; Xichao Ruan *E-mail address:* xichao_ruan@126.com

## Abstract

To fulfill the needs of neutron capture reaction cross-section measurement in keV energy scale in the field of nuclear astrophysics and advanced nuclear energy system development, the 4π $BaF_2$ Gamma-ray Total Absorption Facility (GTAF) developed by the Key Laboratory of Nuclear Data of the China Institute of Atomic Energy (CIAE) has been transplanted and installed at the Back-streaming White Neutron Source (Back-n) of the China Spallation Neutron Source (CSNS) in 2019. A series of results has been achieved and published based on the GTAF since then, and due to which the needs of reducing backgrounds are becoming increasingly urgent. In order to understand the origins of backgrounds and to optimize the facilities, a detailed simulation program using GEANT4 toolkits was established and presented in this paper. To demonstrate the availability of the proved codes, several practical examples of assisting the process of experimental data and helping verify the optimization proposition are also shown in this paper.

**Keywords:** Monte Carlo simulation, Gamma-ray total absorption facility, Neutron Capture cross section, GEANT4, Geometry optimization, White neutron source.

## 1. Introduction

Due to its large cover angle and high detection efficiency, the 4π $BaF_2$ Gamma-ray Total Absorption Facility (GTAF), as shown in Fig.1, is designed to meet the needs of neutron capture cross-section measurement under keV energy scale neutron beams in the topics of nuclear astrophysics and advanced reactor design [1-4].

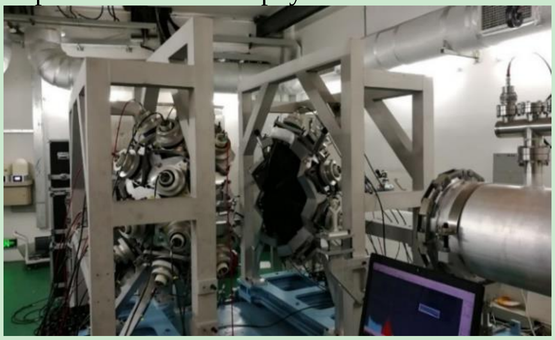

**Fig.1.** GTAF Detector Array and associated facilities installed in the Hall-2 of Back-n CSNS [1]

In order to assist the analysis of experimental data, a set of detailed and reliable Monte Carlo simulation codes is programmed using GEANT4 toolkits [5] as described in the Section 2 and Section 3. A verification by standard library or experimental data is shown in the Section 4 and Section 5 and based on which, several practical examples are presented in the Section 6, including the demonstrations of availabilities in assisting the process of experimental data and in verifying the geometric optimization variants to solve the problems of backgrounds.

## 2. Basis of Detector

### 2.1 Time-of-Flight Method

The Time of Flight (ToF) method is a commonly used method in measuring particles [6,7]. It relies on the principle that the time it takes for a neutron to travel a known distance is inversely proportional to its energy, which could be theoretical calculated in by Equation 1 [6,7].

$$t = \frac{72.3 \times L}{\sqrt{E_n}} \tag{1}$$

where $t$ refers to the flight time, $L$ to the flight distance and $E_n$ to the primary neutron energy.

The measurement of neutron flight time is designed in grand accuracy using specific timing hardware and software system since it is crucial to determine the neutron's energy and to reconstruct the spectrum at the GTAF [8,9].

### 2.2 Multiplicities of $(n,\gamma)$ Reactions

The Multiplicity of reactions is defined as the number of volumes that particles have bypassed with inelastic reactions before being totally absorbed or escaping the sensible crystal array as shown in Fig.2.

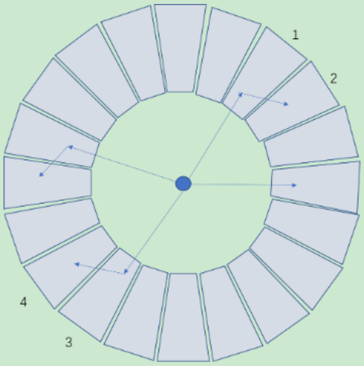


**Fig.2.** Schema of particles multiple reaction in one event in different crystals

It plays a key role in benchmarking valuable information about reaction channels and underlying physics process, such as elastic scattering, inelastic scattering, radioactive capture, etc. since each event has a distinctive multiplicity signature.

### 2.3 Pilled-up Energy of Event Cascades

The de-excitation principle of isotopes in GTAF is shown in Fig.3.

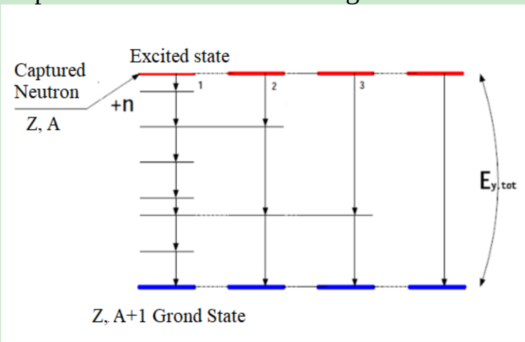


**A** Principle of isotopes de-excitation

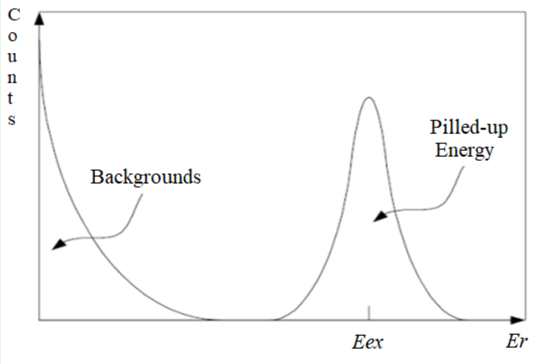


**B** Principle of pilled-up energy

**Fig.3.** Principles of Event Reconstruction [1]

In GTAF, to seek neutron capture reactions is of the most importance since it is one of the key and interest data [1,10]. To distinguish the neutron capture reaction, one of the most practical ways is to find the value of pilled-up released gamma-ray energy $E_{ex}$ since no matter how many reaction channels has been experienced, the $E_{ex}$ remains constant if all data can be restored ideally, as shown in Equation 2.

$$E_{ex} = E_n + Q \tag{2}$$

where the $E_{\mathrm{n}}$ refers to the neutron energy and the $Q$ to the reaction $Q$ value.

## 3. Monte Carlo Simulation

### 3.1 General Idea

As discussed in the Section 1, a reliable Monte Carlo Simulation is needed to be established in order to fulfill the needs of amelioration of facilities and to help of analysis the experimental data.

The reliability of Monte Carlo simulation depends on the details of reconstruction in variety parts, i.e.1) Detailed geometry reconstruction; 2) Accurate physics configurations; 3) Reasonable Calibration and Neutron Beam sources; 4) Capable event reconstruction algorithm and 5) Logical data restoration design.

The GEANT4 simulation toolkits package [5] is chosen as it has been widely used and verified in nuclear physics and high energy physics with strong abilities of extensive physics configurations and mutual geometric reconstruction methods. The kernel version of GEANT4 in use in the simulation of this paper is 11.1.2. The general working flow of the simulation is shown in Fig.4.

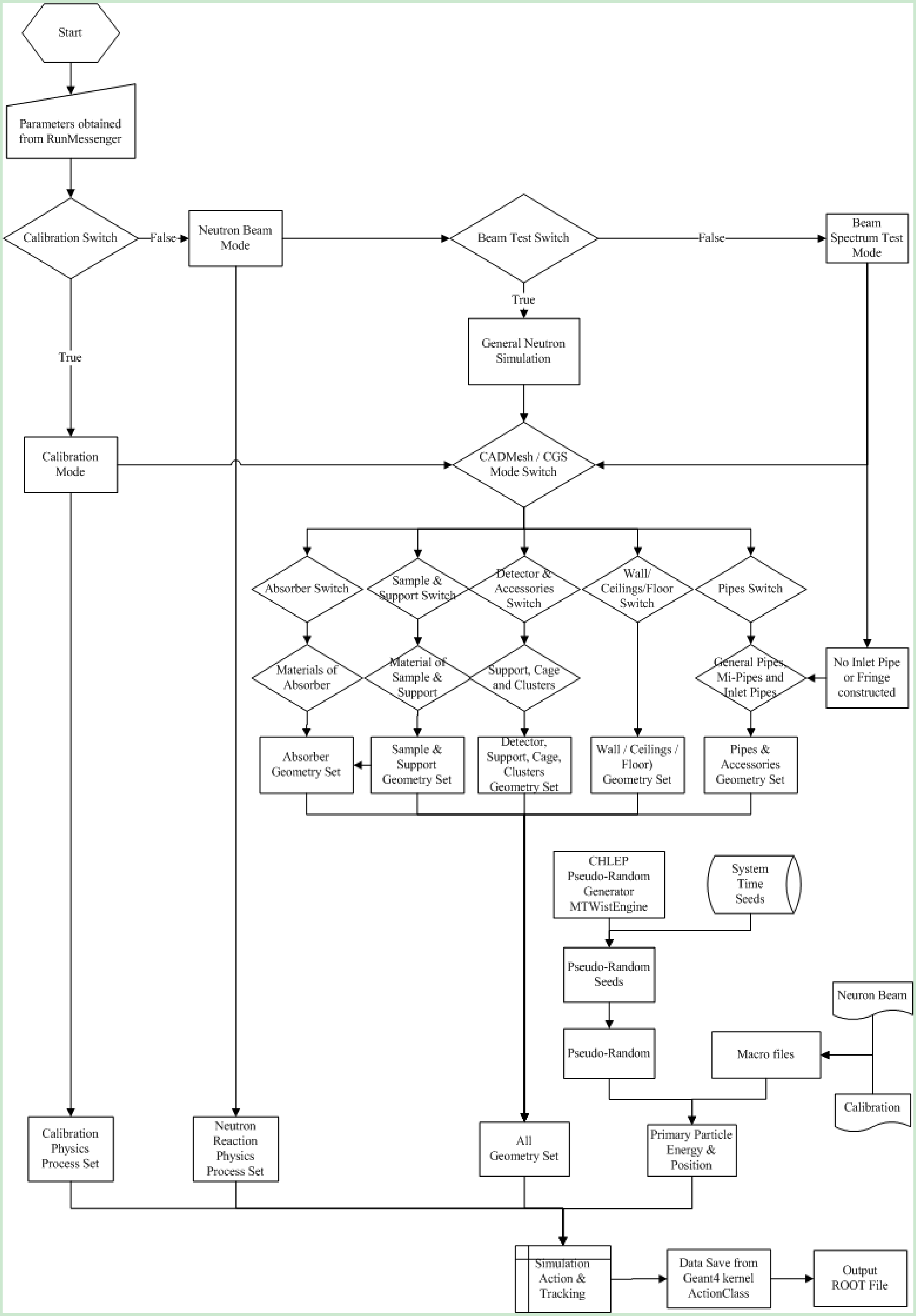


**Fig.4.** General Data Flow of Simulation Codes

## 3.2 Geometry Reconstruction

To adapt to different needs of geometry simulation under certain experimental conditions, different Boolean variables, as shown in Table 1, are offered to users as switches of geometry construction.

**Table 1.**
Boolean variables for Construction under different simulation situation

| Boolean Variables<br>Tier N1 | Tier N2 | Tier N3 | Default |
|---|---|---|---|
| Calibration | / | / | false |
| Beam Test | / | / | false |
| PreConstruction Switch | PreConstruction_Wall | / | false |
| | PreConstruction_GTAF | / | false |
| | PreConstruction_Pipe | / | false |
| | PreConstruction_Absorber | / | false |
| | PreConstruction_ShellSup | / | false |
| | PreConstruction_SampleSup | / | false |
| | PreConstruction_Etagere | / | false |
| General Construct | All Vacuum | / | false |
| | WallConstruct | / | true |
| | BackEnd Trap | / | true |
| Detector Construction | det_Shell | / | true |
| | det_Support | / | true |
| | det_Shelf | / | true |
| | det_Base | / | true |
| | nPartial Crystal Construct | / | true |
| | det_Cluster | / | true |
| Sample Construction | Sample Construct | / | true |
| | | Sample_Au | true |
| | | Sample_C | false |
| | | Sample_Select | false |
| | Sample Support Construct | / | true |
| | | SampleSup_Al | false |
| | | SampleSup_Teflon | true |
| | | SampleSup_Select | false |
| Pipeline Construction | General Pipe | / | true |
| | Penetrate Pipe | / | true |
| | Middle Pipe | / | true |
| Absorber Construction | Absorber Construct | Ab_Select | true |
| Process Analysis | Process Model Mode | / | false |
| | Physics Model Mode | / | true |
| | Simple Canal | / | true |

The geometry is reconstructed to be with the most reasonable details. Apart from the mechanical fabrication errors, the geometric parameters and related materials of the facilities are set as same as the ones measured directly from the actual arrangements in the Back-n of CSNS. In addition to using the Constructed Solid Geometry (CSG) method or the CSG liked methods embedded in GEANT4 toolkits, the subassemblies of the facilities are also reconstructed using CADMesh method [11] as a back-up and agile development option.

The CADMesh is a valuable tool in reconstructing detector constructions in GEANT4 simulations. It allows importing complex geometries created in Computer-Aided Design (CAD) software, with a support of various common ACSII format files, into the GEANT4 simulation program directly.

Although both CSG and CADMesh methods are based on Computer Graphics geometric logics, more preset basic graphics and logical calculation operations are provided by commercial CAD softwares when constructing elements which offer the CADMesh method possibilities of rapid building high level accurate geometric volumes, ensuring that the simulation of detector's physical characteristics could fulfill the crucial needs for obtaining results in particle tracking. It is especially advantageous that the CADMesh method can easily excel at handling complex 3D shapes and curved surfaces when simulating detectors, such as for the GTAF series detectors which contain quite a lot intricate or irregular geometric elements.

According to the topologic definition of different fields in ACSII format CAD files created by FreeCAD [12] in this paper, such as vertex positions, normals, mappings, etc., as shown in Table 2 [12], an interface program is used to read and translate parameters to make the core program of GEANT4 completing the corresponding geometric construction whereas the corresponding materials are defined subsequently by the same way as CSG method in GEANT4.

**Table 2.**
Definition of fields of geometry parameters in ASCII format files

| Field | Meaning | Description |
|---|---|---|
| v | Coordinates of vertices | Definition of a vertex through coordinate x-y-z data in each line. |
| vt | Coordinates of vertex texture | Definition of a vertex texture through coordinate x-y data. |

| Field | Meaning | Description |
|---|---|---|
| vn | List of vertex normal | Definition of normal (number of normals is determined by the intersection of each vertex and face) |
| f | Face | In Computer Graphics, mesh is used as the definition of faces. Every three points on different lines at least with three index values: vertex, vertex texture and normal could define a face. |
| o | Objects | |
| g | Groups | |
| s | Smoothing group | |

The two mentioned methods are designed to be able to switch between each other via a Boolean variable as shown in Table 1.

In addition, for certain elements whose local geometric effect is no need to be detailed considered, the related parameters are calculated and set by an equal-volume factor. For instance, the bellows type BP300 can be considered as a tube with a volume equivalent coefficient of 1.2 while quick release flanges type KF100 would be of 1.47.

The geometric simulation and some of the typical subassemblies are shown in Fig. 5.

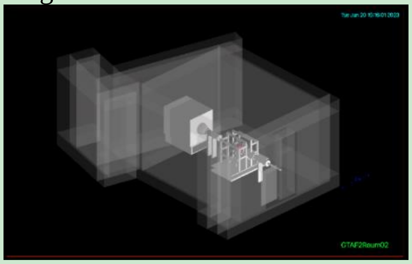

a) Mass Plan of the Hall-2 Geometry using CSG+CAD Method

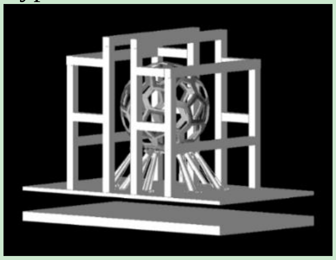

b) Central Zone for the Detector and its associates Geometry using CSG+CAD Method

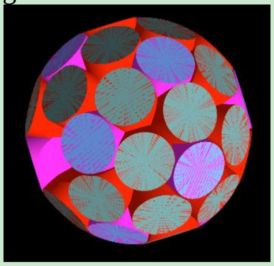

c) $BaF_2$ Crystal Geometry using CSG/CAD Method

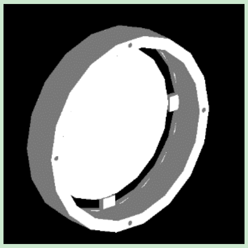

d) Sample Tray/Support Geometry using CSG/CAD Method

e) Bellow Geometry using CSG+CAD Method

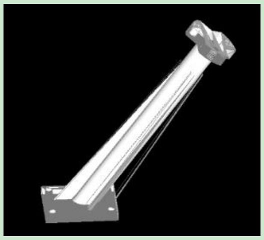

f) Cage Support Geometry using CAD Method

**Fig.5.** Typical Construction of the Hall-2 Environment and Detector Array Geometry

### 3.3 Physics Models

In order to simulate the detector, it is crucial to construct a reasonable physical model.

Considering the simulation under no matter energy calibration mode or neutron beam mode, more interests are concentrated on the response in low energy range, the QGSP_BIC_HP preset physics package [13] is used as a basic physics model package, which contains a series of physics reference including the low-energy reaction, decay, elastic scattering and inelastic processes that can meet the preliminary needs of simulation with results shown in Section 5 in this paper.

The HP type physical process package is used here since the character "HP" refers to High Precision physics models [13] in the context of GEANT4 which provide more accurate and detailed simulations of particle interactions covered with a broader energy range for particles and allowed for more comprehensive simulations of various physics processes.

The preliminary applied physics processes and models are shown in Table 3 and there will be continued to be refined in subsequent work due to different needs of simulation.

**Table 3.**
Applied physics processes and models

| **Physics Model** | **Mode** | |
|---|---|---|
| | **Calib** | **Neutron** |
| QGSP_ BIC_HP | ■ | ■ |
| EMV_option4 | ■ | ■ |
| DecayPhysics | ■ | ■ |
| BiasedRDPhysics | ■ | |
| HardronElasticPhysicsHP | ■ | ■ |
| IonElasticPhysics | ■ | |

| Physics Model | Mode | |
|---|---|---|
| | Calib | Neutron |
| IonPhysics | ■ | |
| GammaNuclearPhysics | | ■ |
| GammaNuclearPhysicsLEND | | ■ (option) |
| NeutronHPPhysics | | ■ |

## 3.4 Primary Sources

Two types of sources, i.e., 1) Calibration sources recommended by the standard library Evaluated Nuclear Data File (ENDF) [14,15]: $^{60}$Co, $^{137}$Cs, and $^{22}$Na; 2) Neutron beams: including a) Neutron beams output from Back-n and b) 4.9eV mono-energetic neutron beams, are reconstructed using specific macro files, in which contains a histogram of spectral and spatial parameters and related normalized weighting coefficients to provide the required information for the simulation of primary sources.

### 3.4.1 Calibration Sources

Three Calibration Sources recommended by ENDF library, $^{60}$Co, $^{137}$Cs and $^{22}$Na, are reconstructed in the simulation with the same geometric parameters as used in real experiments [16]. The dimensions are set as $\phi 32\times 4$mm, $\phi 32\times$ 4mm and 25×25mm respectively.

### 3.4.2 Neutron Sources

Two neutron beam sources, mono-energetic neutron beams and spectral neutron beams are simulated.

Due to the time-resolution limit of hardware in real experiments, Time-of-Flight (ToF) spectrum of beams with initial energy over 1 MeV cannot be well resolved. Therefore, on the first stage of simulation, an upper energy limit of 1 MeV has been set to both of the options [16]. The matrix of neutron energy spectrum and initial momentum spectrum is written in a macro file.

**a.** The mono-energetic neutron beams are simulated with parameters of a 4.9 eV mono-energy and a spatial Beam spot obtained from the CMOS experiment data at the Back-n of CSNS. It is used for obtaining a clear image of the largest resonant cross-section of the standard $^{197}$Au sample which leads to verify the reliability of the codes and to be used to help calculate the theoretical efficiency or other required information.

**b.** The spectral neutron beams are simulated with the same spectral and spatial characteristics of which from the Back-n. It is used for the analysis of backgrounds and for the calculation of the theoretical neutron capture cross-section of samples. The simulated beam spot is shown in Fig.6.

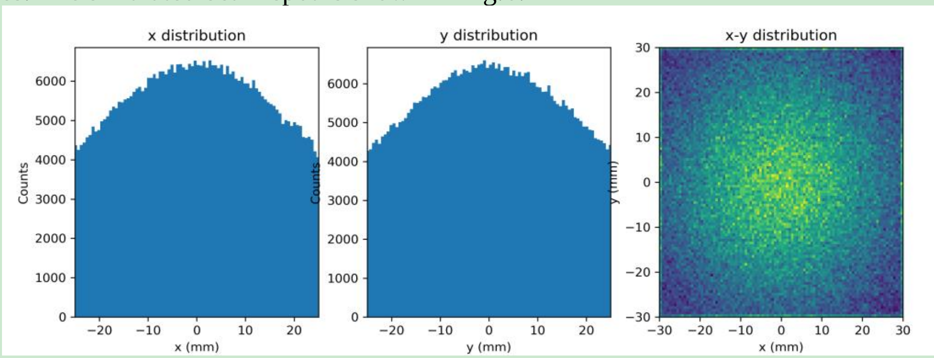


**Fig.6.** Simulation of Neutron Beam Spot at Back-n of CSNS

### 3.4.3 Pseudo-random Number Generator

The statistical properties of Pseudo-Random Number Generator (PRNG) have a great impact on the reliability of Monte Carlo simulation results. There are several popular candidate PRNGs for nuclear physics, as the James Random, Mersenne Twister and Ranlux64.

The MTWistEngine pseudo-random number generator [17] is chosen as the PRNG used in the simulation due to two main reasons, as:

1) a big enough pool of valid pseudo-random number of $2^{19937}$-1 can be generated at one single operation which might support the needs of an upper limit of about $2 \times 10^9$ events in each run in GEANT4 toolkits and might also fulfill the potential needs for further study using the accumulated simulation data;

2) a high reliability since it has been passed almost all the rigorous random number tests referred to the analysis thesis in reference [18-20].

In order to get the system beeper via an I/O data channel as initial seeds feeding the pseudo-random generator, a time seed interface program is designed, programmed and linked to the EventAction class of the simulation program.

## 3.5 Simulation Run and Action Classes

Under no matter the Calibration mode or the Neutron Beam mode, the simulation can be started by emitting the primary particles by calling the detail parameters of the initial particles in the macro file (including the initial energy, initial momentum, and initial position) and the specific operation mode defined in the RunMessenger interface, via the General Particle Sources (GPS) function embedded in GEANT4.

After emission, the behavior of particles depends on the different physical models and definitions of the physical processes in Section 3.3 while travelling through various spatial volumes in the geometry described in Section 3.2 and performs to cutoff or truncate the information according to the demands in the various action classes.

According to the design logic of action classes built-in GEANT4, each Run consists of the number of Events defined in the macro file, and in each Event, according to the setting of the particle step length and physical process, the corresponding Step is included, and the required information can be filtered through the action classes of Stack and Track.

At the end of each Run, i.e. after the last Event, the corresponding data and information will be saved and output according to the required format preset in RunMessenger.

# 4. Primary Data Analysis Program

In order to meet the basic pre-processing requirements of the simulation data, a general data processing program with a set of Qt-based GUI interface is designed and tested.

## 4.1 GUI Interface

In order to facilitate the implementation of commonly used data preliminary processing functions, a visual human-machine GUI interface through Qt version 5.9.7 is designed, as shown in Fig.7.

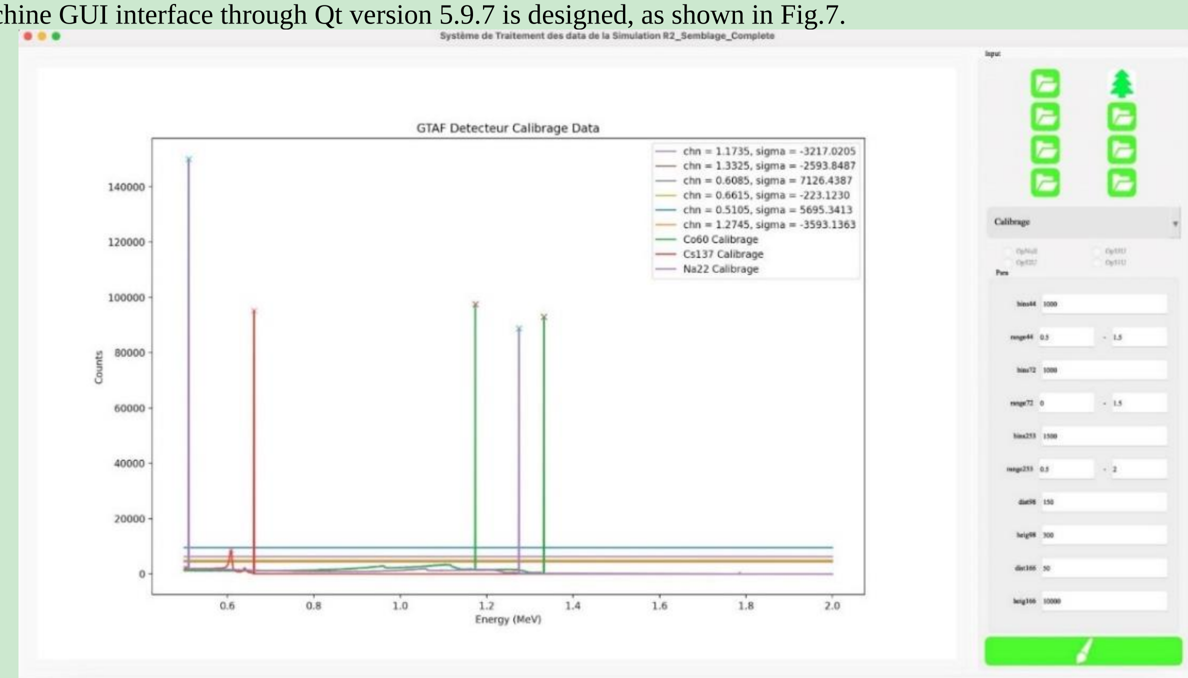


**Fig.7.** GUI Interface of GTAF Simulation Pre-processing Program

Through PythonQt and PyRoot, the commonly used functions are realized by transporting the data flow via various interface, including the import and export of files in various basic format, switching between neutron beam mode and calibration mode, display and fitting functions of energy spectrum and ToF spectrum.

The visualization program uses the control of Qt and realizes the data interface required to call the above functions, and realizes the basic data preliminary processing,

### 4.2 Reconstruction Algorithm of Event Cascades

The simulation can be done by each event, or each run as required. Consistent with the process of experimental data processing, two general and basic event reconstruction algorithm subprograms in the data processing program are designed: energy reconstruction and position reconstruction.

The reconstruction is relatively simpler in the simulation since it is possible to retrieve the target data directly from GEANT4 built-in functions. Particles are transported and tracked via the functions of Action Classes in the framework of GEANT4 toolkits until they are absorbed in certain volumes or escape the set cut-off areas.

The essential value, as the deposition energy, the time-of-flight, the multiplicities, the geometric volumes, the material, the reaction channel, and other relevant information can be taken from and recorded after each step or event. Meanwhile, the corresponding data of each reaction channel can be distinguished by calling the physics model or physics process of each track.

#### 4.2.1 Energy reconstruction

The deposited energy could be traced in each step of particles transportation with help of build-in algorithms of GEANT4 which makes one of the privileges of processing simulations data compared to the counterpart of experiment data is that the pilled-up energy peaks and event cascades reconstructions are much easier to be done.

The particles are designed to be transported via the functions of action class in each Step until they are absorbed in certain volumes or escape the preset cut-off areas. While the simulation runs, each particle will be labeled by each generation, the associated information of particles would be transferred via a user-set personalized function to the TrackingAction class in order to get further processed.

Considering that the simulation results of interest are those with responses in the detector array, the geometric volume information is of more importance. Therefore, a label each volume number (the CopyID) are recorded at the same time.

For situations where further processing of energy deposition is not required, the above-extracted data can be directly transferred from the SteppingAction class to the EventAction class so as to be accumulated and stored directly. And after which, the data would be finally passed to the Analyzer for saving in a certain format according to the designed dataflow shown in Fig.4.

On the other hand, where there is a need for further processing, a TrackingAction class retains interface functions for users to filter the specific required deposition energy is designed. According to the needs of the user's simulation objectives, data can be transferred to the Analyzer after preliminary processed in the TrackingAction class, where more preprogrammed reorganization tools, such as different reaction channels, different multiplicities, and different areas to store and reconstruct the required energy spectrum, are set as to be described in the Section 4.3.

The original simulation data output from the dataflow above are saved by separate detector crystals. The reconstructed energy spectrum can be output directly in the form of divided crystals, or according to the user's needs, a deposited energy spectrum reconstruction output in the unit of the total detector can be achieved in the form of the sum of the total deposition data of each crystal in the same Event.

The above functions can be implemented in the RunMessenger by adjusting relative Boolean variables, or through GUI tabs. Thus, after each Run, the energy spectrum of particles could be reconstructed.

#### 4.2.2 Time-of-Flight Spectrum Simulation

In order to verify the results with experimental data, the flight time of particles is designed to be recorded in the simulation.

The very start time point T0 is preset in the EventAction class at the beginning of Event when the primary particles begin to emit in every loop. When triggered in each Step (under SteppingAction mode) or in each Sensitive Detector zone (under SensitiveDetector mode), the corresponding time is recorded and saved in a tuple or histogram predeclared in the RunAction class. Note that the recorded time mentioned above is a Global Time in the entire Event since T0 is the beginning of each Event. Right at the end of each Event, corresponding time data are recorded in different tuples or trees in the ROOT files through the pre-selection conditions in action classes of each Step, Track, Stack or Event. Therefore, a ToF Spectrum can be generated at the end of the whole Run, e.g., the end of the final Event.

In addition, similar to processing of experimental data, the corresponding simulated energy spectrum (E-ToF) can be calculated using the flight length of particles and the simulated ToF spectrum through the mentioned Equation 1. The flight length of particles is obtained by adding the flight distance in each Step. It is calculated in geometric simulation program and transferred to the analysis functions by two following ways which can be switched into each other by users through a Boolean variable.

**1)** Calculated by extracting the geometric length of the corresponding passing geometric elements in the Detector Construction source file, and the very geometric parameters would be transferred to the Analyzer source file through the transfer function;

**2)** Calculated directly in Step action class through the built-in variable function of GEANT4 toolkit, whereafter the step length would be passed to the function in the Event action class in order to store and generate the E-ToF spectrum directly.

### 4.2.3 Position reconstruction

Similar to the reconstruction of ToF spectrum, the position information (3-Dimensions vector tuple) of each step can be traced and recorded while the deposited energy (the difference between the pre-step and post-step energy) in dedicated geometric volumes is not equaled to zero in the SteppingAction class.

## 4.3 Reorganization Tools

### 4.3.1 Multiplicities

During the experiment installation setup stage, as discussed in the Section 2.2, a proper design should be considered for processing and identification the multiplicities. In GTAF, an electronic circuitry based on NOT gate circuit of nuclear electronics technology is realized with several key parameters well set including the energy and timing thresholds to identify particle interactions.

In the simulation program, a similar but of more precision and practical method has also been applied. Technically, the multiplicities of each Event are counted by the number of different CopyIDs of geometric volumes that the deposit energy is not equal to zero before the particle is fully absorbed or escapes from the sensible arrays since there is a unique CopyID tagged to each of the geometric volumes reconstructed in the simulation codes.

### 4.3.2 Reaction Channels

In experimental data processing, distinguishing data from different reaction channels is the core algorithm of data processing, which is realized through different gates in order to help understand the experimental data and phenomena.

In simulation, the physical process occurred at each step could be traced before or after each step. In order to avoid the null Pointer error in C++ coding environment, apart from the usual protection by a judgement function, the post step physics model filter is used in this program. A string value, with a Pronouns preset in GEANT4 or by users-set to the dedicated physics model or physics process, due to the Boolean values switch that has been chosen in the RunManager, would be returned. After transferred to the Stack and Track classes of the simulation program, the string values of the relevant physics processes or physics models are passed to the Analyzer and stored in the corresponding tuple or other format in a ROOT file.

After the simulation is completed, the value of the physics processes or physics models could be called in Primary Data Analysis Program, and the ToF spectrum or energy spectrum involved in different reaction channels can be classified and plotted.

## 4.4 Spectrum Broadening and Semi-automatic Peak Finding

### 4.4.1 Broadening of the Energy Spectrum

Since GEANT4 cannot simulate the nuclear electronic effect in the preset physical process, the ratio of electronic response is obviously 100%. Thus, the simulated data need to be broadened before supporting the experimental data analysis.

In the preliminary analysis program, Gaussian's function is used as the broadening algorithm. The specific process of the broadening algorithm is as follows:

1) Determine the total normalized bin number and the corresponding coordinate value of the corresponding spectrum (or the corresponding segment of the spectrum);
2) Determine an energy resolution that is set according to the experiment or set by the user;
3) Determine the width of the error limit;
4) Determine the constant of Gaussian broadening: by ensuring that the integral of Gaussian broadening with the above parameters is the same as the original count value;
5) Plotting and recording the parameters.

### 4.4.2 Semi-automatic Fitting and Peak Finding

Spectrum fitting and peak finding are generally performed in the range of interest when processing data. The semi-automatic spectrum fitting, and peak finding process can be implemented in the primary data analysis program.

The algorithm of spectrum fitting, and peak finding is similar to the counterpart of energy spectrum broadening, which is also achieved by fitting with Gaussian function with a series of basic initial parameters, including the approximate region of the peak position, basic fitting adjustment parameters, etc. that could be modified and fitted directly in the GUI interface mentioned in Section 4.1.

The peak position and the final coefficient of the fitting iteration will be displayed in the display area of the GUI interface or be printed in the Terminal, which will be stored and be used for subsequent data analysis.

## 5. Validation of Reliability

### 5.1 Responses to Calibration Source

Three simulated calibration sources mentioned in the Section 3.4 are designed to validate the reliability of the geometric simulations and the algorithm of reconstruction. The results are shown in Fig.8, in which the peaks of piled-up deposit energy are all in good agreement with data from ENDF library that well demonstrates the reliability of the geometry and physics configurations.

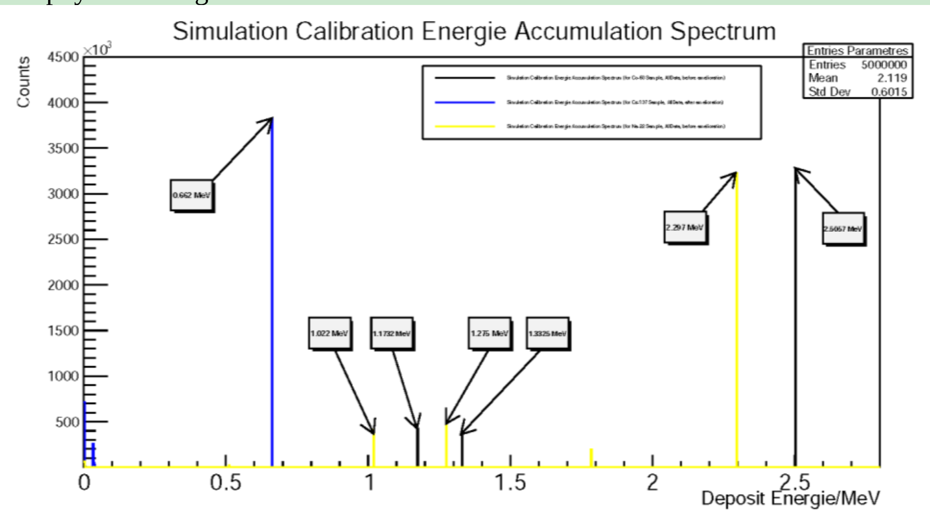


**Fig.8.** Calibration Results of Simulation

In addition, preliminary processing of multiplicities and reunited-$BaF_2$ crystals event reconstruction is performed for the simulation data. Taking the simulation data of $^{60}Co$ source calibration as an example, two gamma-rays with energy of 1.17 MeV and 1.33 MeV respectively, emit spontaneously. The pilled-up energy of 2.5 MeV could be a benchmark to evaluate the efficiency of the detector array as discussed in the Section 3.6, as shown in Fig.9.

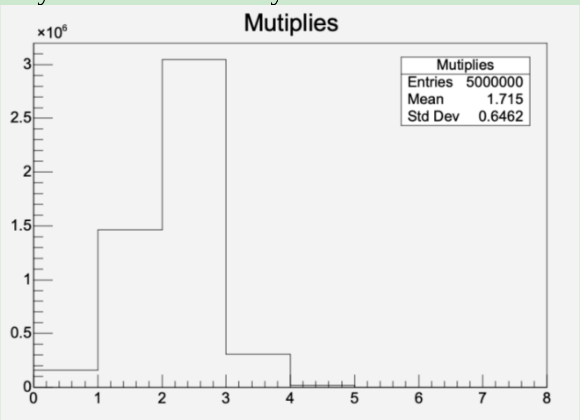


**a)** Simulated Multiplicities distributions of $^{60}Co$ source

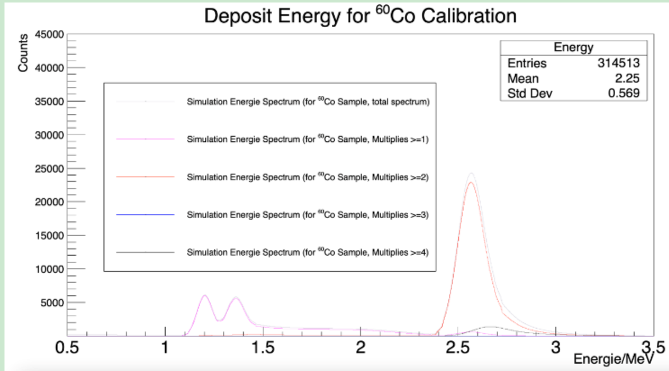


**b)** Energy Spectrum in different Multiplicities filters conditions

**Fig.9.** Demonstration of Multiplicities identification for $^{60}Co$ source simulated Calibration experiment

It could preliminarily be proved that the geometric reconstruction of the simulation program is effective, and the basic reconstruction algorithm is available. At present, the experimental data processing of GTAF is still ongoing and the control results from the experiment sides would be published in consequence.

## 5.2 Response to Neutron Capture Reaction

Considering that there is a very large resonant neutron capture cross-section at 4.9 eV of the isotope $^{197}Au$, which is several orders of magnitude larger than other cross-sections such as elastic scattering, the very specific monoenergetic neutron beam is commonly used for verifying the physics configurations of the simulation.

To this end, a 4.9 eV monoenergetic neutron beam with the same geometric spatial distribution as the Back-n neutron source starts from the vacuum tube 72.7 m up away the sample tray and a standard thin cylindrical $^{197}Au$ Sample with a same geometric dimension as experiment, i.e. a thickness of 0.2 mm and a diameter of 40 mm, is simulated.

In this simulation, a lower energy threshold of $10^{-2}$ eV is preset for each simulated crystal unit to facilitate preliminary data processing. The response information of particles on the $BaF_2$ crystal was recorded as described in the Section 4.2 and after which, the energy spectrum and ToF spectrum were output through event reconstruction.

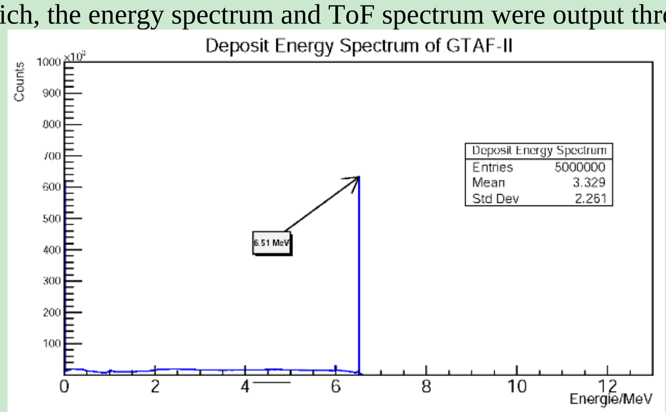


a) Deposited Energy Spectrum

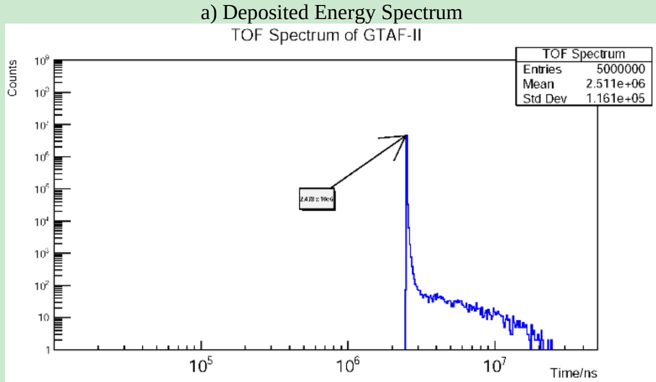


b) ToF Spectum

**Fig.10.** Simulation Result of $^{197}Au$ Sample response to the 4.9 eV Monoenergetic Neutron Beam

As shown in Fig.10, a peak of deposited energy around 6.51 MeV and a typical time peak of $2.478 \times 10^6$ ns are clearly shown in the Energy Spectrum and in the ToF Spectrum respectively, which are consistent with the standard values and demonstrated well the validation of the simulation codes.

# 6 Practical examples

## 6.1 Assistant Processing and Understanding Experimental Data

### 6.1.1 Impact of Different Neutron Beam Energy

In order to speed up the simulation and considering the characteristics of electronic devices in real experiment, the Back-n neutron beam energy segment below 1MeV is often used as the input neutron beam source.

However, neutron beams in different energy bands may have different effects on the background [21]. To confirm the influence of the high-energy band on the part of the effect of interest, four different initial input neutron beam sources are simulated respectively, with Effect-Background Ratio results shown in Table 4.

**Table 4.**
Theoretical Effect-Background ratio under different simulation beam conditions

| Number of Simulation | Neutron Beam Condition: Energy Spectrum | Neutron Beam Condition: Spatial Structure | Effect-Background Ratio |
|---|---|---|---|
| N_04 | Back-n Energy Spectrum (filter under 1MeV) | Back-n Spatial Structure | 7.26% |
| N_29 | Back-n Energy Spectrum | Back-n Spatial Structure | 7.11% |

As can be seen from the above table, although the high-energy segment has a certain influence on the spectral structure, it has little effect on the key data, as the background-effect ratio. Therefore, when using simulation calculations for rough analysis, a simplified neutron source term, with a filter of under 1MeV energy spectrum, can be used to improve the computational efficiency.

### 6.1.2 Discrimination data by different Reaction Channels

The Discrimination of different reaction channels is one of the most privilege to use the simulation codes since it could provide an ideal panorama of all reactions occurred. A demonstration of this function is shown in Fig.11.

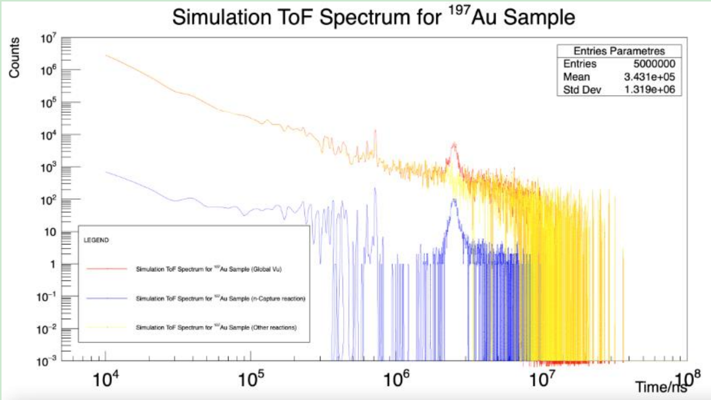


a) ToF Spectrum (Different Reaction Channels)

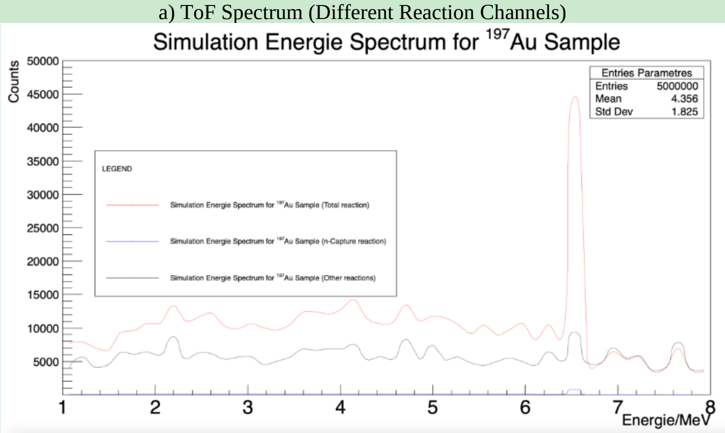


b) Energy Spectrum (Different Reaction Channels)

**Fig.11.** Demonstrations of Reaction Channels Discrimination

By realizing the function, theoretical neutron capture reaction detecting efficiency can be calculated. Besides, it is an important analysis tool to provide possibilities to help better understand the phenomena of experimental data and optimize the structure by reducing the background impact.

## 6.2 Assistant in Evaluation of Preliminary Geometric Optimization

### 6.2.1 Theoretical Analysis of Background

In order to support the coming upgrade of the facilities, the theoretical backgrounds could be analyzed with the help of the simulation codes.

According to Fig.11, a series of abnormal resonant peaks displayed in the ToF spectrum ranged from $8 \times 10^5$ ns to $1.1 \times 10^6$ ns. The preceding geometric volumes and related materials of the abnormal data are traced by the simulation codes, as shown in Fig.12.

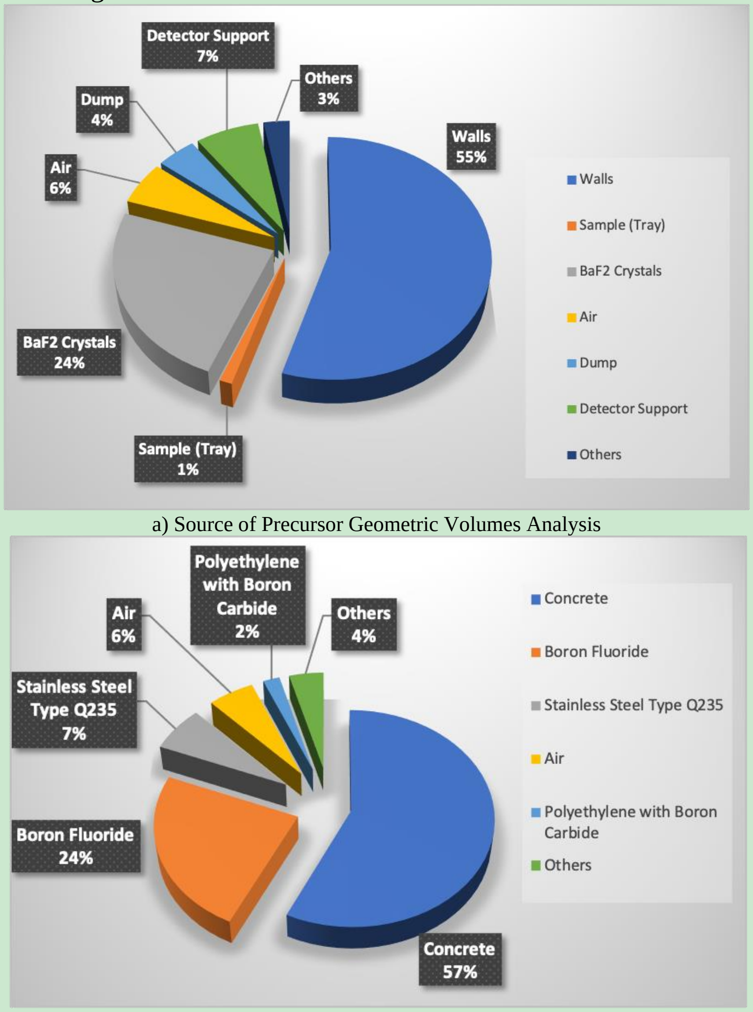


a) Source of Precursor Geometric Volumes Analysis



b) Source of Precursor Material Analysis

**Fig.12.** Demonstration of Primary Analysis of Background

Considering that most of the precursor origins of the background are the concrete-made volumes (walls, ceilings, and floors), a preliminary proposition of optimization thus could be made as one possible proposition to reduce the impact of abnormal backgrounds is to isolate the scattering sub-particles caused by the wall, the ceiling, and the floor from neutron beamline, especially from the central area where the crystal array lied.

### 6.2.2 Evaluation of Geometric Optimization Proposition

One potential structural optimization option is to add a vacuum tube in the central area (i.e., the area through the center of detector array) with a ball-shaped neutron absorber outside the sample tray/support, as shown in Fig.13.

The simulation results for the combination of different pipe diameters and materials are summarized in Table 5, which show that the addition of the central vacuum pipe and the absorber outside the sample tray can significantly help to reduce the influence of the anomalous background.

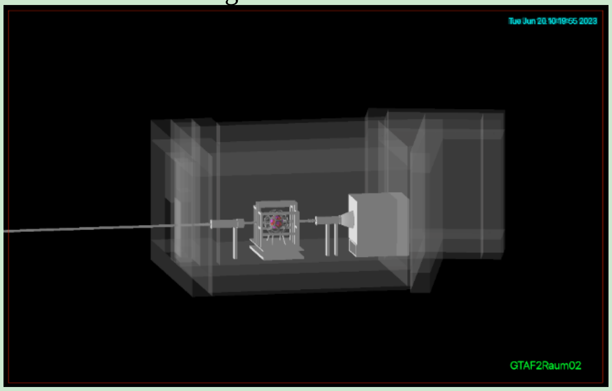

a) Mass Plan with the optimized structural

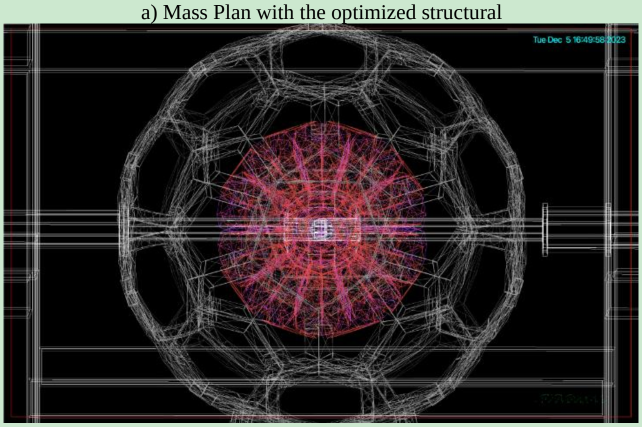

b) Detail simulation of the optimization structure

**Fig.13.** Mass Plan with the optimized structural

**Table 5.**
Theoretical Effect-Background ratio of simulation under different optimization conditions

| **Number of Simulation** | **Central Pipe** | | **Absorber outside Sample Tray** | | **Effect-Background Ratio** |
|---|---|---|---|---|---|
| | **Material** | **Dimension** | **Material** | **Dimension** | |
| N_04 | N/A | N/A | N/A | N/A | 7.26% |
| N_08 | Stainless Steel 304 | $\phi 51$ | Polyethylene (30% boron carbide) | $\phi 51$ | 15.87% |
| N_09 | Aluminum Alloy 6061 | $\phi 52$ | | $\phi 52$ | 15.31% |
| N_10 | | $\phi 55$ | | $\phi 55$ | 16% |

Obviously, the final optimization of structure would be decided after considering more details and analysis. Validation experiments of absorbing layers are prepared to be done, and after which all the simulated and experimental data would be verified in the very near future.

## 7. Summary

A Monte Carlo simulation program for GTAF based on GEANT4 toolkits is established and verified in this paper which allows us to use it assisting the analysis of experimental data and helping optimize the facilities.

The geometry of the entire facilities is reconstructed in great detail according to the as-build drawings and the actual layout conditions on site. Together with reasonable physics configurations and event reconstruction algorithms, the codes have been tested and validated by comparing simulated with experimental data of three types of calibration sources and two types of neutron beam sources. All of the comparison results show positive agreements which demonstrate the reliability of the codes created.

Two types of typical application examples are presented at the end of this paper to show some commonly scenarios where the above codes can be applied.

More work will be done to enforce the performance of the codes and more applicable scenarios will be executed to help data analysis and other requests by the proved simulation codes.

## Fundings

Project supported by the National Natural Science Foundation of China (N$^{o.}$ 11975317, 11975318 and 12275363), the Key Laboratory of Nuclear Data Foundation (N$^{o.}$ JCKY2022201C158), Continuous-Support Basic Scientific Research Project (N$^{o.}$ BJ010261223282).

## References


[1] Luan Guangyuan et al, Experiment and Simulation of Detection Efficiency of Gamma-ray Total Absorption Facility. Journal of Isotopes, 35(4), 273-280 (2022).

[2] SHI Bing et al, Online method for neutron capture reaction cross-section measurement. Atomic Energy Science and Technology, 52(9), 1537-1544 (2018).

[3] Zhang Qiwei et al, Cross section measurement of neutron capture reaction based on HI-13 tandem accelerator. Power Laser and Particle Beams, 33(4), 0440 (2021).

[4] Zhang Qiwei et al, Acta Phys. Sin. 70222801 (2021).

[5] Agostinelli et al, GEANT4 — A simulation toolkit. Nuclear instruments and methods in physics research section A: Accelerators, Spectrometers, Detectors and Associated Equipment 506.3, 250-303 (2003).

[6] Copley, J. R., Udovic, T. J.. Neutron time-of-flight spectroscopy. Journal of research of the National Institute of Standards and Technology, 98(1), 71 (1993).

[7] Klempt W, Review of particle identification by time-of-flight techniques. Nuclear Inst. and Methods in Physics Research, A, 433, 1 (1999).

[8] Zhang Qiwei et al, Data Acquisition System Based on Gamma-ray Total Absorption Facility. Atomic Energy Science and Technology, 50(3), 536-540 (2016).

[9] Zhang Qiwei et al, Study of Waveform Analysis and Timing Method for Gamma-ray Total Absorption Facility. Atomic Energy Science and Technology, 48 (Suppl1), 70-75 (2014).

[10] Zhang Qiwei et al, Study of Neutron Shield and Absorber for Gamma Total Absorption Facility. Nuclear Physics Review, 37(3), 771-776 (2020).

[11] Poole, C. M. et al, A cad interface for Geant4. Australasian physical $\&$ engineering sciences in medicine, 35, 329-334 (2012).

[12] Gayer D, O'Sullivan C et al, FreeCAD visualization of realistic 3D physical optics beams within a CAD system-model. Millimeter, Submillimeter, and Far-Infrared Detectors and Instrumentation for Astronomy VIII. SPIE, 9914, 745-758 (2016).

[13] Wright, D. H. et al, AIP Conference Proceedings, Vol. 896, No. 1, pp. 11-20, American Institute of Physics, March 2007.

[14] Thermal Neutron Capture $\gamma$'s (CapGam), https://www.nndc.bnl.gov/capgam. Accessed 27 Oct 2023.

[15] Evaluated Nuclear Data File, https://www.nds.iaea.org/exfor/endf.htm. Accessed 07 Oct 2022.

[16] Ren Jie et al. Simulation of the background of experimental end-stations and the collimator system of the CSNS back-streaming white neutron source. Nuclear Techniques, 37(10), 110521 (2014).

[17] Makoto Matsumoto $\&$ Takuji Nishimura. Mersenne twister: a 623-dimensionally equi-distributed uniform pseudo-random number generator. ACM Transactions on Modeling and Computer Simulation (TOMACS), 8 (1), 3–30 (1998).

[18] Martirosyan, N.et al, Spectral test of the MIXMAX random number generators. Chaos, Solitons & Fractals, 118, 242-248 (2019).

[19] Sepehri, F. et al, Selection of random number generators in GATE Monte Carlo toolkit. Nuclear Instruments and Methods in Physics Research Section A: Accelerators, Spectrometers, Detectors and Associated Equipment, 973, 164172 (2020).

[20] Tsvetkov, E. A., Empirical tests for statistical properties of some pseudorandom number generators.

Mathematical Models and Computer Simulations, 3, 697-705 (2011).
[21] Zhang Qiwei et al, Calibiration of Neutron Detection Efficiency of Li-glass Detector. Nuclear Physics Review, 30(2): 99-103 (2013).

## Figure Legends

Fig. 1 GTAF Detector Array and associated facilities installed in the Hall-2 of Back-n CSNS

Fig. 2 Schema of particles multiple reaction in one event in different crystals

Fig. 3 Principles of Event Reconstruction

Fig.4. General Data Flow of Simulation Codes

Fig.5. Typical Construction of the Hall-2 Environment and Detector Array Geometry

Fig.6. Simulation of Neutron Beam Spot at Back-n of CSNS

Fig.7. GUI Interface of GTAF Simulation Pre-processing Program

Fig.8. Calibration Results of Simulation

Fig.9. Demonstration of Multiplicities identification for $^{60}Co$ source simulated Calibration experiment

Fig.10. Simulation Result of 197Au Sample response to the 4.9 eV Monoenergetic Neutron Beam

Fig.11. Demonstrations of Reaction Channels Discrimination

Fig.12. Demonstration of Primary Analysis of Background

Fig.13. Mass Plan with the optimized structural

## Figures

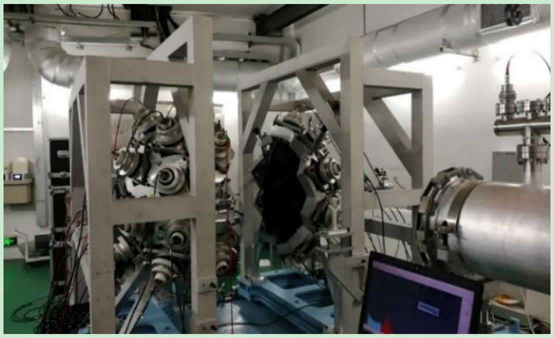

**Fig.1.** GTAF Detector Array and associated facilities installed in the Hall-2 of Back-n CSNS [1]

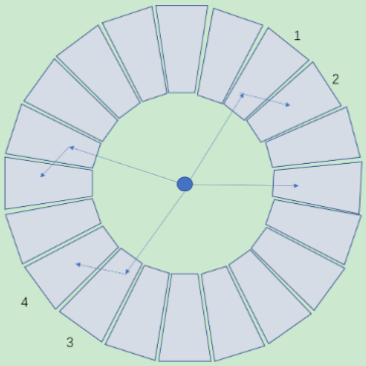

**Fig.2.** Schema of particles multiple reaction in one event in different crystals

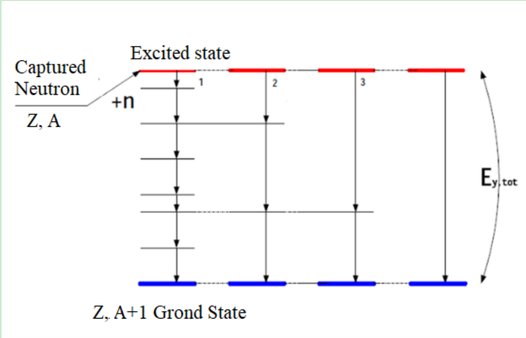


**A** Principle of isotopes de-excitation

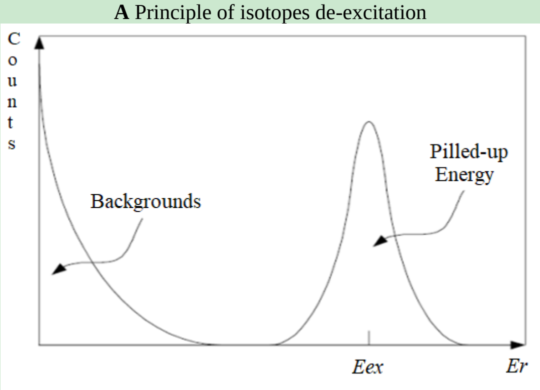


**B** Principle of pilled-up energy

**Fig.3.** Principles of Event Reconstruction [1]

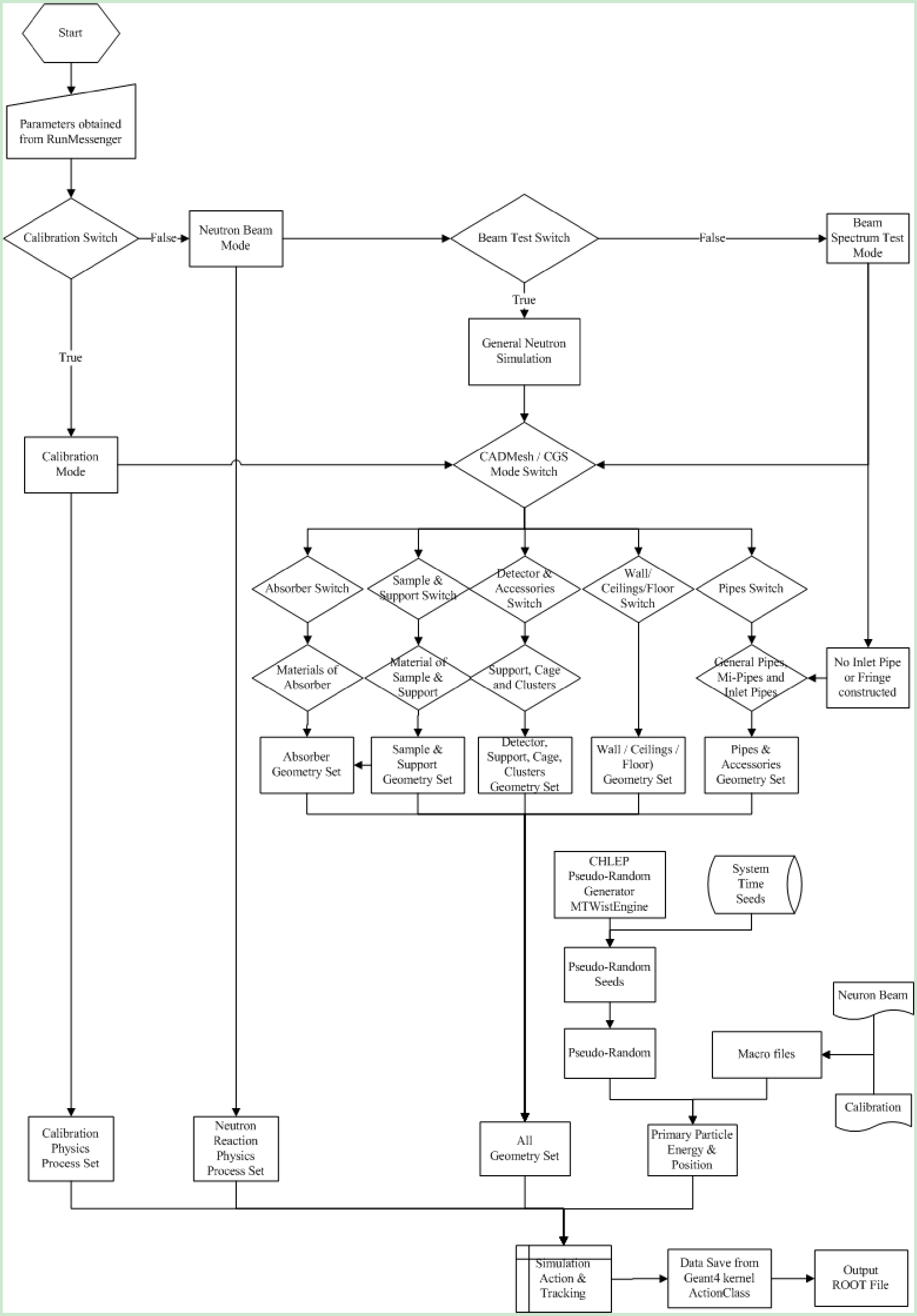


**Fig.4.** General Data Flow of Simulation Codes

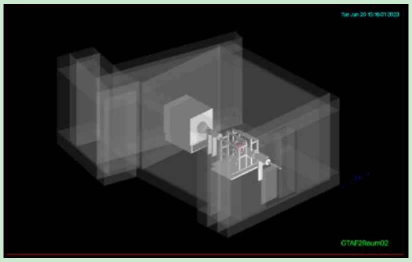

a) Mass Plan of the Hall-2 Geometry using CSG+CAD Method

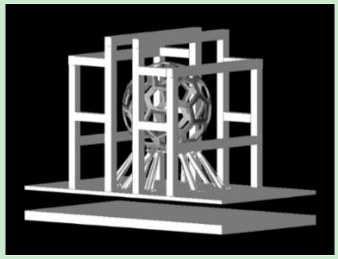

b) Central Zone for the Detector and its associates Geometry using CSG+CAD Method

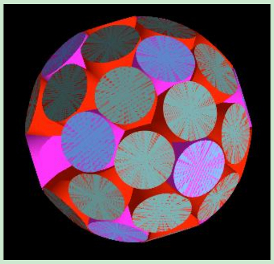

c) $BaF_2$ Crystal Geometry using CSG/CAD Method

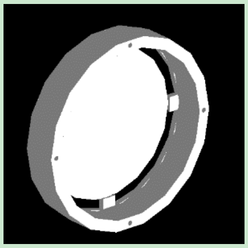

d) Sample Tray/Support Geometry using CSG/CAD Method

e) Bellow Geometry using CSG+CAD Method

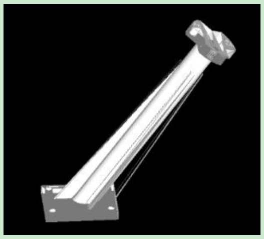

f) Cage Support Geometry using CAD Method

**Fig.5.** Typical Construction of the Hall-2 Environment and Detector Array Geometry

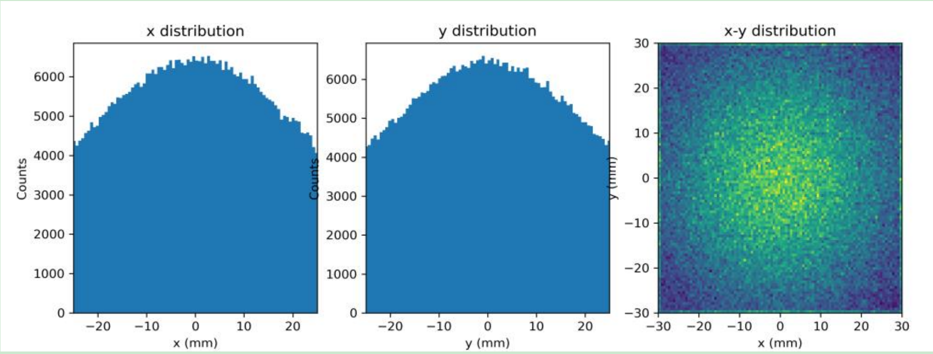

**Fig.6.** Simulation of Neutron Beam Spot at Back-n of CSNS

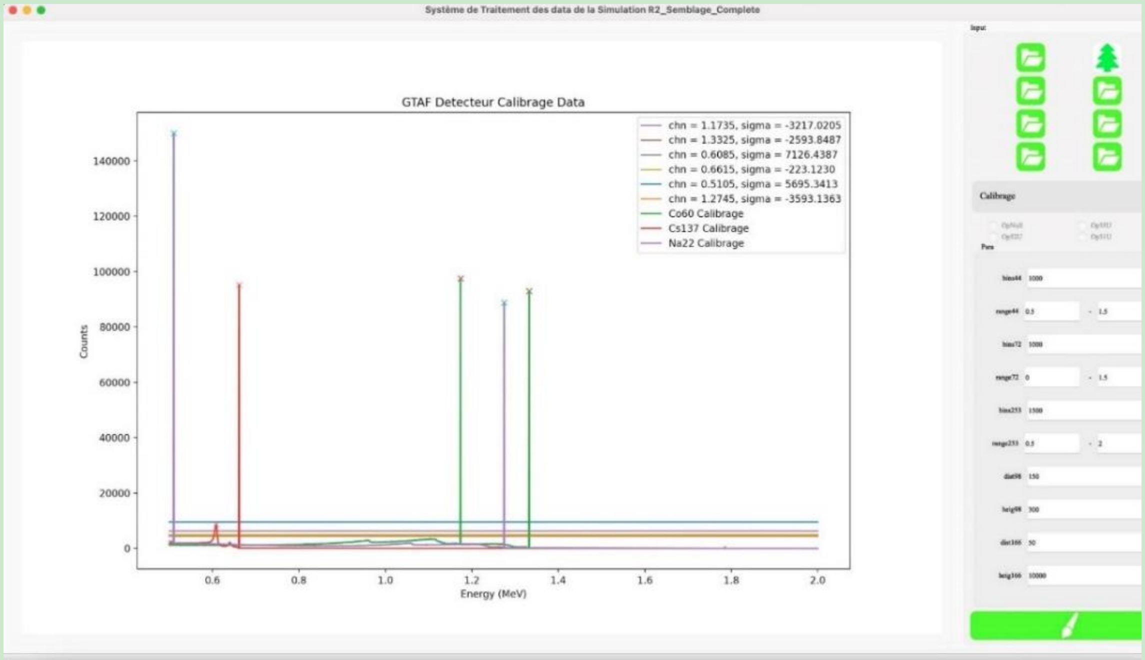


**Fig.7.** GUI Interface of GTAF Simulation Pre-processing Program

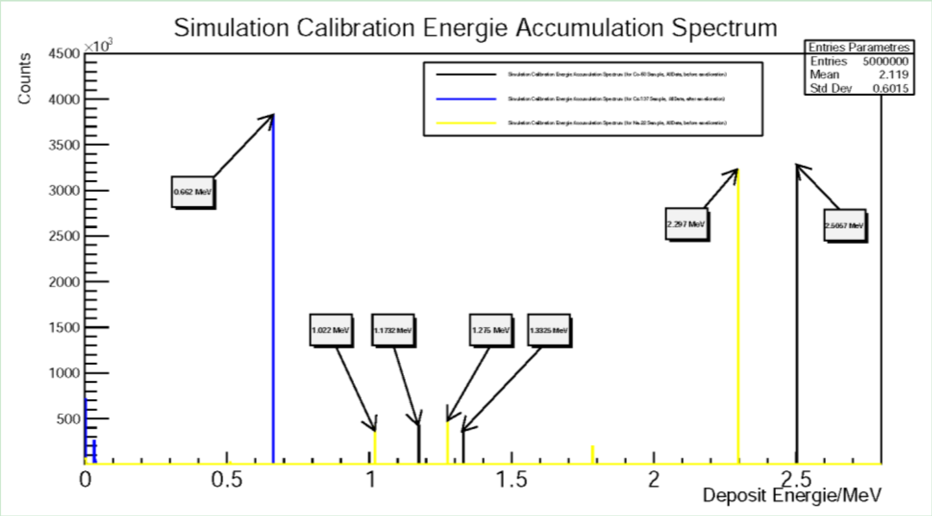


**Fig.8.** Calibration Results of Simulation

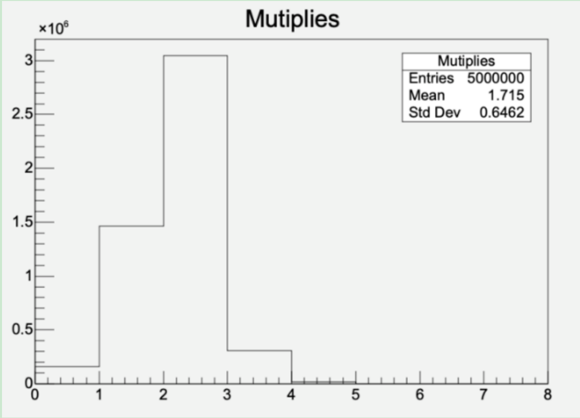


**a)** Simulated Multiplicities distributions of $^{60}Co$ source

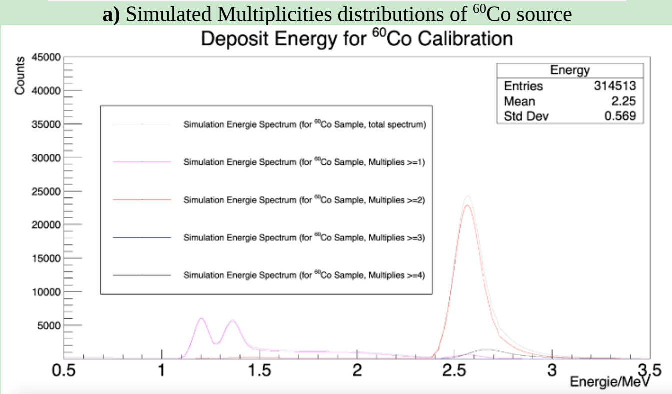


**b)** Energy Spectrum in different Multiplicities filters conditions

**Fig.9.** Demonstration of Multiplicities identification for $^{60}Co$ source simulated Calibration experiment

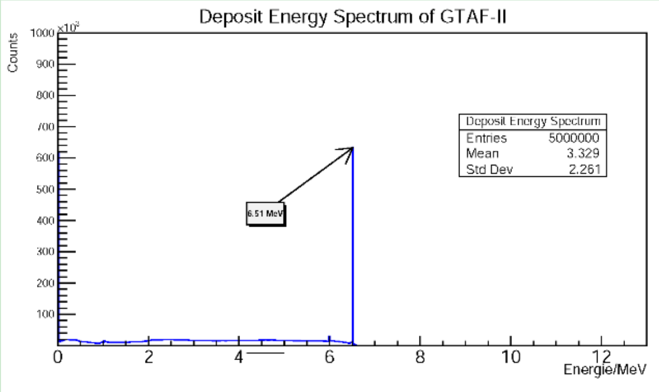


a) Deposited Energy Spectrum

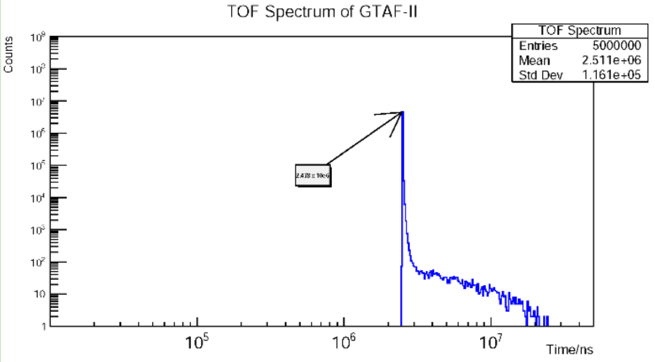


b) ToF Spectum

**Fig.10.** Simulation Result of $^{197}$Au Sample response to the 4.9 eV Monoenergetic Neutron Beam

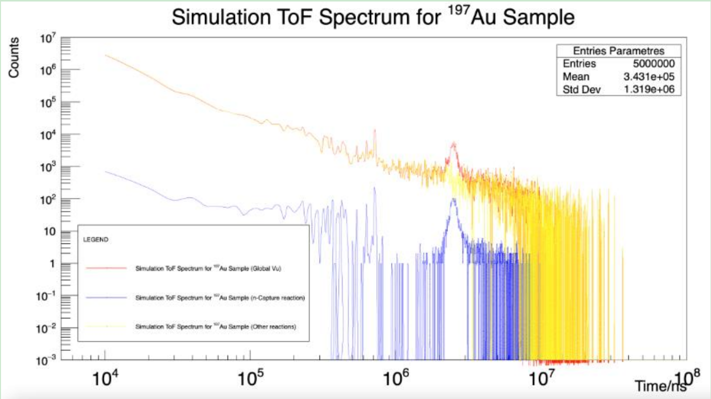


a) ToF Spectrum (Different Reaction Channels)

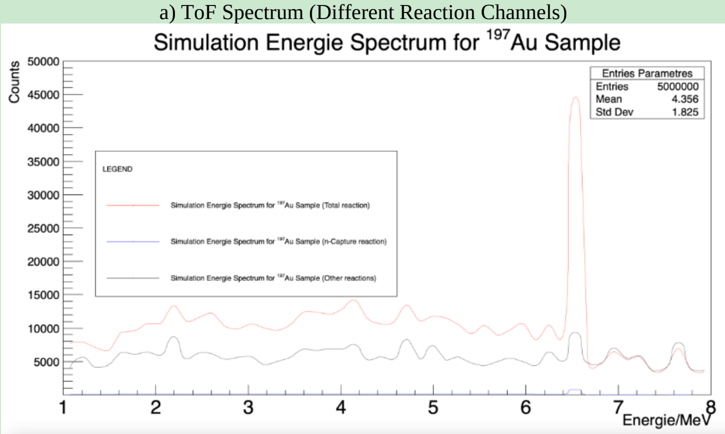


b) Energy Spectrum (Different Reaction Channels)

**Fig.11.** Demonstrations of Reaction Channels Discrimination

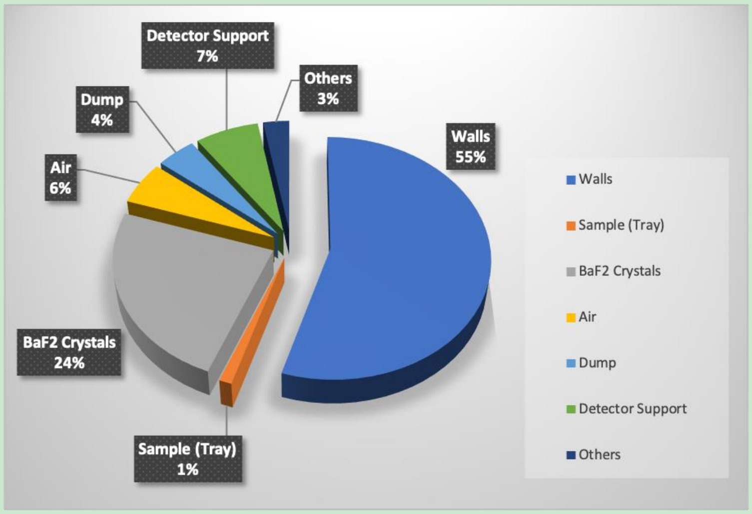


a) Source of Precursor Geometric Volumes Analysis

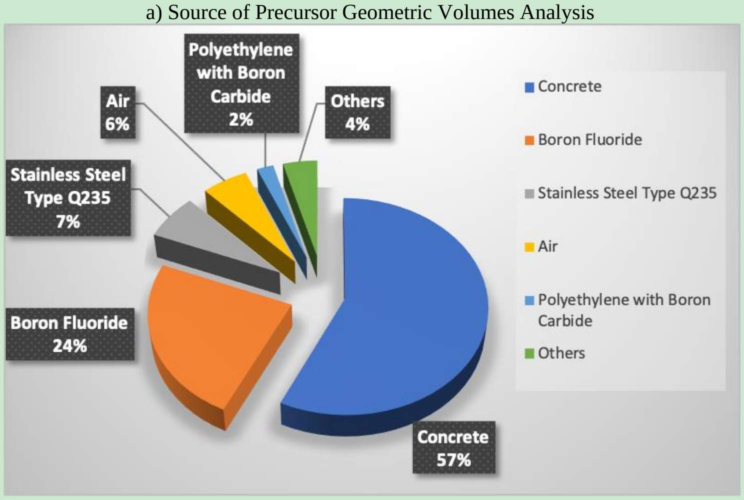


b) Source of Precursor Material Analysis

**Fig.12.** Demonstration of Primary Analysis of Background

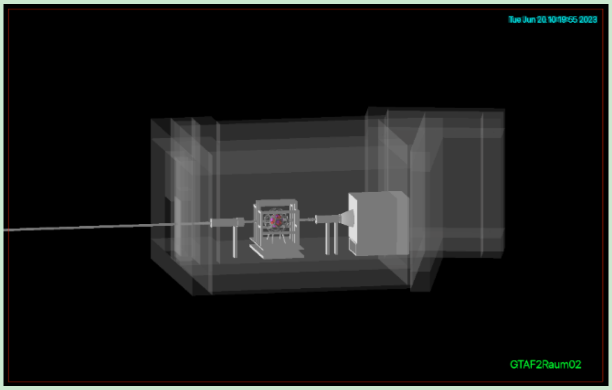

a) Mass Plan with the optimized structural

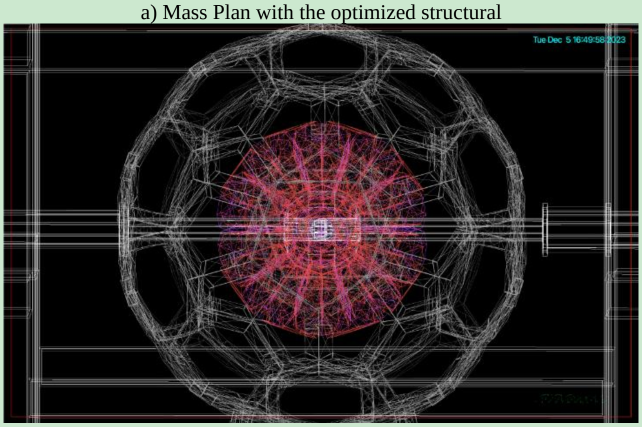

b) Detail simulation of the optimization structure
**Fig.13.** Mass Plan with the optimized structural

# Tables

**Table 1.**
Boolean variables for Construction under different simulation situation

| Boolean Variables<br>Tier N1 | Tier N2 | Tier N3 | Default |
|---|---|---|---|
| Calibration | / | / | false |
| Beam Test | / | / | false |
| PreConstruction Switch | PreConstruction_Wall | / | false |
| | PreConstruction_GTAF | / | false |
| | PreConstruction_Pipe | / | false |
| | PreConstruction_Absorber | / | false |
| | PreConstruction_ShellSup | / | false |
| | PreConstruction_SampleSup | / | false |
| | PreConstruction_Etagere | / | false |
| General Construct | All Vacuum | / | false |
| | WallConstruct | / | true |
| | BackEnd Trap | / | true |
| Detector Construction | det_Shell | / | true |
| | det_Support | / | true |
| | det_Shelf | / | true |
| | det_Base | / | true |
| | nPartial Crystal Construct | / | true |
| | det_Cluster | / | true |
| Sample Construction | Sample Construct | / | true |
| | | Sample_Au | true |
| | | Sample_C | false |
| | | Sample_Select | false |
| | Sample Support Construct | / | true |
| | | SampleSup_Al | false |
| | | SampleSup_Teflon | true |
| | | SampleSup_Select | false |
| Pipeline Construction | General Pipe | / | true |
| | Penetrate Pipe | / | true |
| | Middle Pipe | / | true |
| Absorber Construction | Absorber Construct | Ab_Select | true |
| Process Analysis | Process Model Mode | / | false |
| | Physics Model Mode | / | true |
| | Simple Canal | / | true |

**Table 2.**
Definition of fields of geometry parameters in ASCII format files

| Field | Meaning | Description |
|---|---|---|
| v | Coordinates of vertices | Definition of a vertex through coordinate x-y-z data in each line. |
| vt | Coordinates of vertex texture | Definition of a vertex texture through coordinate x-y data. |
| vn | List of vertex normal | Definition of normal (number of normals is determined by the intersection of each vertex and face) |
| f | Face | In Computer Graphics, mesh is used as the definition of faces. Every three points on different lines at least with three index values: vertex, vertex texture and normal could define a face. |
| o | Objects | |
| g | Groups | |
| s | Smoothing group | |

**Table 3.**
Applied physics processes and models

| Physics Model | Mode | |
|---|---|---|
| | Calib | Neutron |
| QGSP_ BIC_HP | ■ | ■ |
| EMV_option4 | ■ | ■ |
| DecayPhysics | ■ | ■ |
| BiasedRDPhysics | ■ | |
| HardronElasticPhysicsHP | ■ | ■ |
| IonElasticPhysics | ■ | |
| IonPhysics | ■ | |
| GammaNuclearPhysics | | ■ |
| GammaNuclearPhysicsLEND | | ■ (option) |
| NeutronHPPhysics | | ■ |

**Table 4.**
Theoretical Effect-Background ratio under different simulation beam conditions

| **Number of Simulation** | **Neutron Beam Condition** | | **Effect-Background Ratio** |
|---|---|---|---|
| | **Energy Spectrum** | **Spatial Structure** | |
| N_04 | Back-n Energy Spectrum (filter under 1MeV) | Back-n Spatial Structure | 7.26% |
| N_29 | Back-n Energy Spectrum | Back-n Spatial Structure | 7.11% |

**Table 5.**
Theoretical Effect-Background ratio of simulation under different optimization conditions

| Number of Simulation | Central Pipe | | Absorber outside Sample Tray | | Effect-Background Ratio |
|---|---|---|---|---|---|
| | Material | Dimension | Material | Dimension | |
| N_04 | N/A | N/A | N/A | N/A | 7.26% |
| N_08 | Stainless Stell 304 | $\phi 51$ | Polyethylene (30% boron carbide) | $\phi 51$ | 15.87% |
| N_09 | Aluminum Alloy 6061 | $\phi 52$ | | $\phi 52$ | 15.31% |
| N_10 | | $\phi 55$ | | $\phi 55$ | 16% |